

# NOE, a Neutrino Oscillation Experiment at Gran Sasso Laboratory

Paolo Bernardini <sup>\*</sup>, Giancarlo Barbarino <sup>†</sup> and Fausto Guarino <sup>†</sup>

(*NOE* Collaboration)

<sup>\*</sup> Dipartimento di Fisica dell'Università and INFN  
via per Arnesano, 73100 Lecce, Italy

<sup>†</sup> Dipartimento di Scienze Fisiche dell'Università and INFN  
via Cintia, 80126 Napoli, Italy

## Abstract

The project of a large underground experiment (*NOE*) devoted to long baseline neutrino oscillation measurement is presented. The apparatus is composed by calorimetric modules interleaved with TRD modules and has been optimized to be sensitive in the region of  $\sin^2 2\theta$  and  $\Delta m^2$  suggested by the atmospheric neutrino oscillation signal.

## 1 Introduction

The first version of the *NOE* proposal has been submitted to the Gran Sasso Scientific Committee in February 1996 [1]. From that time on, many efforts (technical design, tests, simulations and so on) have been done to improve the project, in terms of scientific goals, detector performances and granularity, safety and reduction in costs [2, 3, 4]. Here a brief progress report is presented, mainly devoted to describe the latest developments with respect to [5].

The scientific goal of *NOE* long baseline (LBL) experiment is the measurement of neutrino masses looking for  $\nu_\mu \rightarrow \nu_e$  and  $\nu_\mu \rightarrow \nu_\tau$  oscillations. The strategy of *NOE* design is to have oscillation sensitivity by looking for the  $\tau$  decay ( $\nu_\mu \rightarrow \nu_\tau$  oscillation) or for an electron excess ( $\nu_\mu \rightarrow \nu_e$  oscillation) and by measuring a deficit of muons in apparent NC/CC ratio.

The major experimental hint for the  $\nu$  oscillation search in the region of low  $\Delta m^2$  ( $10^{-3} \div 10^{-2} \text{ eV}^2$ ) comes from the muon deficit observed in atmospheric neutrino flux measurements [6, 7, 8]. Recent results from LBL reactor neutrino experiment (CHOOZ) exclude neutrino oscillation in  $\bar{\nu}_e$  disappearance mode in the range  $\sin^2 2\theta > 0.18$  for large  $\Delta m^2$  [9].

Given the confirmations of the atmospheric neutrino anomaly and the negative CHOOZ result, a LBL experiment has to fulfill the following requirements:

1.  **$\nu_\tau$  tagging.** The search for  $\nu_\tau$  appearance becomes fundamental in order to confirm the oscillation phenomenon. This search requires detector high performances to reveal the  $\tau$  decay in different channels.
2. **Measurement of the ratio NC/CC.** This robust and unambiguous test is mandatory to investigate on the existence of a neutrino oscillation signal. Moreover in a scenario, never ruled out, in which a neutrino oscillates in a sterile neutrino the oscillation can be discovered only by measuring a deviation from expected NC/CC ratio. There is no doubt that this measurement can be done only with a massive detector.
3. **Atmospheric neutrinos.** After the last results which suggest smaller values of  $\Delta m^2$ , the interest for the atmospheric neutrinos is raised up. It would be interesting to test this effect using a massive apparatus based on a different technique with respect to the water Čerenkov detectors.
4. **Fast response.** If a beam from CERN to Gran Sasso will be available in the next years, a strong competition with American and Japanese LBL programs is foreseen: at present, the 7 kton *NOE* project can adequately compete with the 8 kton MINOS detector and with K2K.

According to these remarks the *NOE* program can be summarized in this way:

- Direct  $\nu_\tau$  appearance by kinematical  $\tau$  decay reconstruction and inclusive (NC/CC)  $\nu_\mu$  disappearance.
- Investigation of  $\nu_\mu \rightarrow \nu_e$  oscillation in a mixing angle region two orders of magnitude beyond the CHOOZ limit.
- Atmospheric neutrino studies.

In order to improve the  $\nu_\tau$  search, the apparatus has been implemented with Transition Radiation Detector (TRD) interleaved between calorimetric modules (CAL). The combination of TRD and CAL informations strongly enforces  $e$ ,  $\mu$ , and  $\pi$  identification, thus permitting the study of the  $\tau$  decay. In particular the  $\tau \rightarrow e\nu\nu$  channel is detectable with a clean signature because of the low background (residual  $\nu_e$  beam). Moreover the good electron identification in the TRD and the low  $\pi^0$  background allow to reach high  $\sin^2 2\theta$  sensitivity looking for  $\nu_\mu \rightarrow \nu_e$  oscillation, thus considerably enlarging the region investigated by CHOOZ.

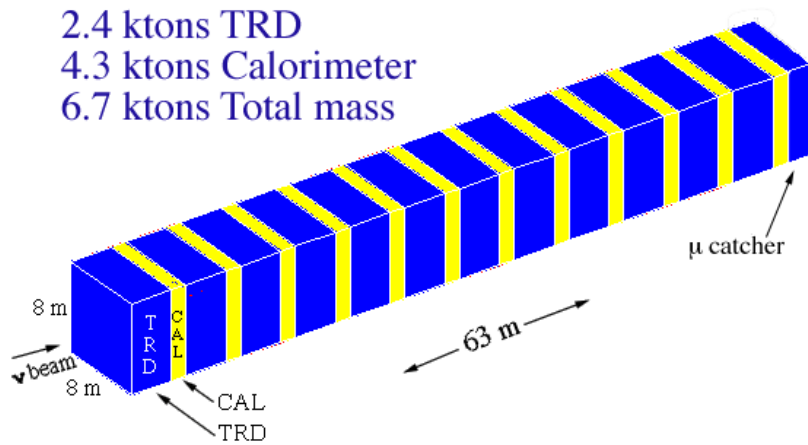


Figure 1: Schematic view of the  $NOE$  detector

## 2 The $NOE$ detector

The detector (Fig. 1) is a classical fixed target apparatus consisting of a sequence of 12 modules. Each one is composed by a lighter part (TRD target) in which vertex,  $e$ -identification and kinematics are defined, followed by a fiber scintillating calorimeter devoted to absorb the event and to measure the energy. The Basic Module (BM) is shown in Fig. 2. Appearance measurement is performed on the events generated in TRD (2.4 *kton*), disappearance measurement on all events (generated in  $\sim 7$  *kton* of target).

The calorimetric element is an 8 *m* long bar having iron ore and scintillating fibers<sup>1</sup> suitably distributed inside and parallel to the axis. The calorimetric module is made by alternate planes of crossed bars. The calorimetric bar consists of more logical cells with square cross section, the iron/iron-ore volume ratio is 0.3. The iron ore is radiopure and practically cost free.

At present the latest production developments of 2 *mm* diameter scintillating fibers provides an attenuation length of 4.5 *m* and an increase in light yield of 10÷15 %. These figures allow to build 8 *m* long bars. Further investigations to improve fiber features are in progress because longer fibers shall permit to enlarge the  $NOE$  cross section ( $9 \times 9$  *m*<sup>2</sup>) and mass (8 *kton*). It is worth noting the very high intrinsic granularity of the proposed calorimeter : the average distance between the fibers inside the absorber is of the order of 3 *mm*. In a simple and often used way, all fibers are grouped together at each side of the calorimetric bar and sent to single or multipixel photodetector.

The TRD module consists of 32 vertical layers of  $8 \times 8$  *m*<sup>2</sup> area, each made by polyethylene foam radiator ( $\rho \sim 100$  *mg/cm*<sup>3</sup>) and 256 proportional tubes ( $3 \times 3$  *cm*<sup>2</sup> cross section), filled with an *Ar* (60%) - *Xe* (30%) - *CO*<sub>2</sub> (10%) mixture, already tested in MACRO experiment. Consecutive layers have tubes rotated of 90°.

A graphite wall of 5 *cm* thickness is set in front of each of the first 24 layers of the TRD module acting as a 174 *ton* target for  $\nu_e$  and  $\nu_\tau$  interactions, to be identified in the following layers. The last target wall is followed by 8 TRD layers in order to identify the secondary particles. Each target wall corresponds to 0.25  $X_0$  while the

<sup>1</sup>Extruded scintillator strips with wavelength shifter fibers have been also studied.

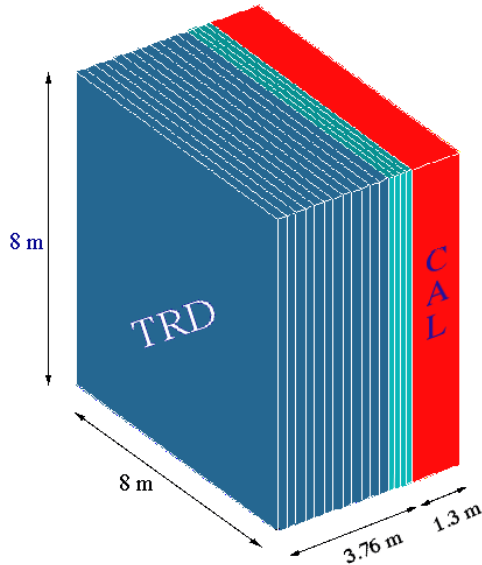


Figure 2: The Basic Module of the  $NOE$  detector

entire TRD basic module corresponds to about  $7 X_0$  and  $3.5 \lambda_I$ . The total length is about  $3.76 m$ .

So many layers of proportional tubes permit to determine the muon energy by means of multiple measurements of energy loss  $dE/dx$ . Combining informations coming from both subdetectors (TRD and CAL) the discrimination between  $e$ ,  $\mu$  and  $\pi$  is largely enforced allowing the study of several channels for the neutrino oscillation signature.

### 3 $\nu_\tau$ appearance and requirements about $\nu$ beam

The rate of  $\nu_\tau$  CC events is given by

$$R_\tau = A \int \sigma_\tau P_{osc} \Phi dE, \quad (1)$$

where  $E$  is the energy,  $\sigma_\tau$  the  $\nu_\tau$  CC cross section,  $P_{osc}$  the oscillation probability,  $\Phi$  the muon neutrino flux and  $A$  the number of target nucleons in the detector. The search for  $\nu_\tau$  requires that the term  $\sigma_\tau P_{osc} \Phi$  is large. Therefore a dedicated  $\nu$ -beam has to provide most of its flux in the energy range where the factor  $\sigma_\tau P_{osc}$  is larger.

Assuming the mixing of two neutrinos, the oscillation probability results

$$P_{osc} = \sin^2 2\theta \sin^2(1.27 \Delta m^2 L/E), \quad (2)$$

where  $L = 731 km$  is the distance CERN – Gran Sasso. CC cross section as a function of energy is shown in Fig. 3 for  $\nu_\mu$  and  $\nu_\tau$ . We have to note that the  $\tau$  cross section grows slowly with energy above a threshold of about  $3.5 GeV$ . The factor  $\sigma_\tau P_{osc}$  is shown in Fig. 4 for different values of  $\Delta m^2$ . The optimal energy is about  $15 GeV$  for  $\Delta m^2 = 0.01 eV^2$  and decreases gently with  $\Delta m^2$  towards a limiting value of about  $10 GeV$ .

As an example the number of  $\nu_\tau$  CC interactions per  $10^{19}$  protons on target per  $kton$  has been calculated for different proposed beams [10, 11, 12] whose spectra are shown in Fig. 5. The rate of  $\nu_\tau$  CC interactions is shown in the first plot of Fig. 6 as

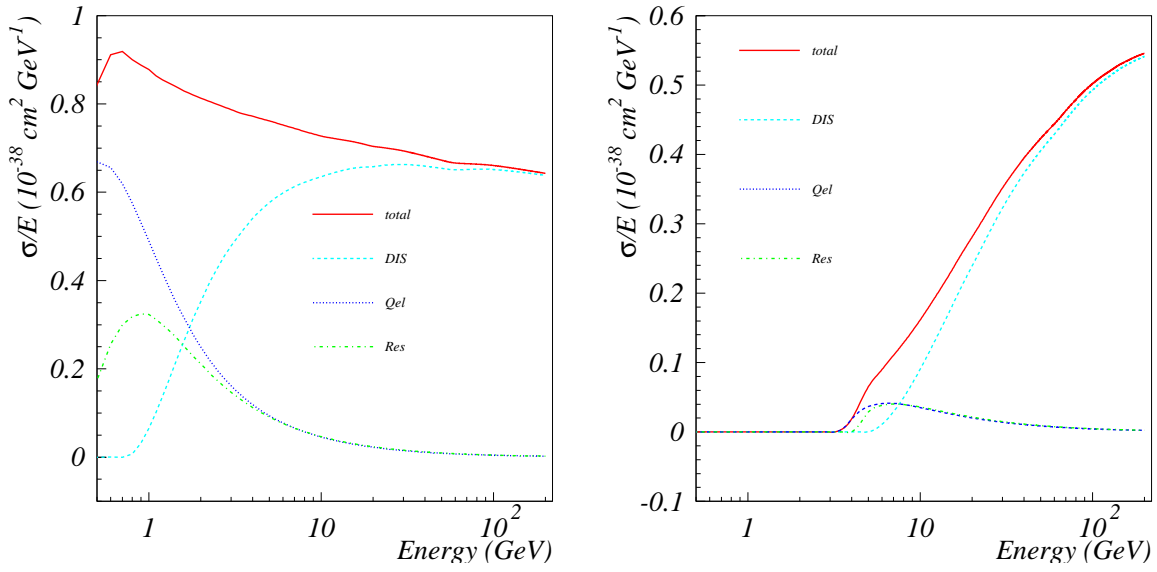


Figure 3: Ratio of  $\nu_\mu$  and  $\nu_\tau$  CC cross section over energy.

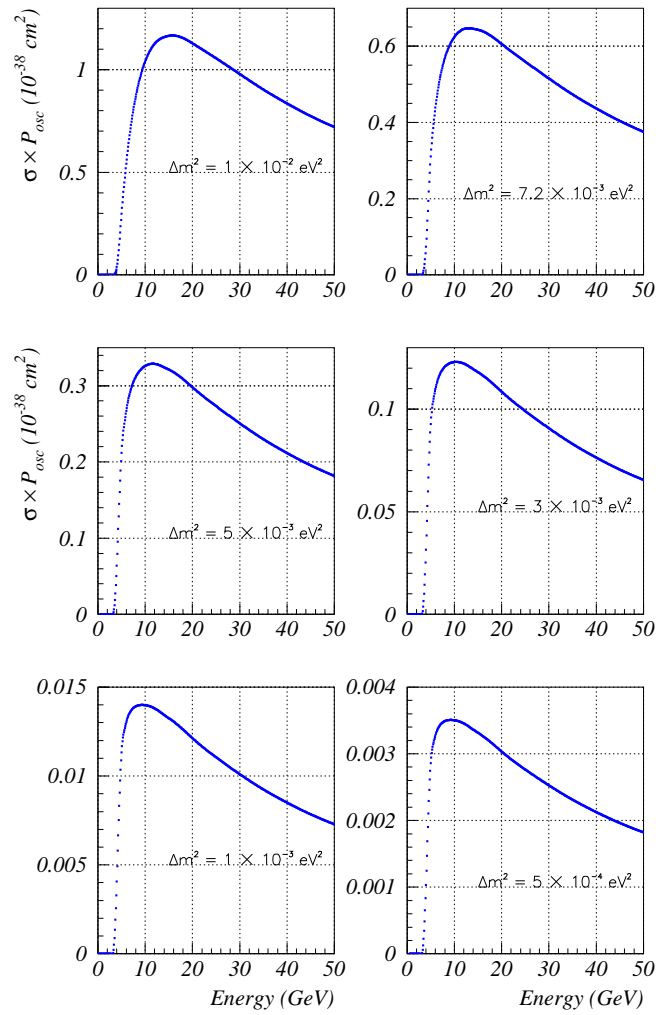


Figure 4:  $\nu_\tau$  CC cross section multiplied by the oscillation probability for different values of  $\Delta m^2$ .

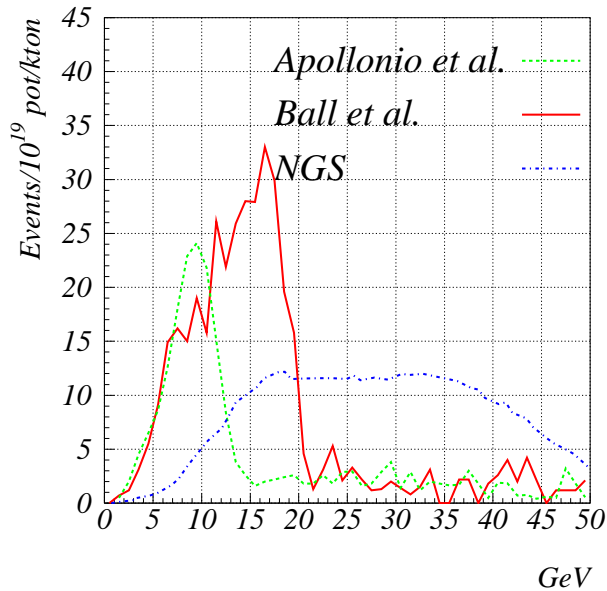


Figure 5:  $\nu_\mu$  CC interaction spectra for different proposed beams.

a function of  $\Delta m^2$ . The highest  $\tau$  yield is obtained with a beam like that proposed by Ball *et al.* [10], narrowly peaked around an energy that better matches the appearance requirements.

Fig. 6 shows also the rate of residual  $\nu_\mu$  CC interactions. From comparison of the plots in Fig. 6 we observe that the beam of Ref. [10] has a higher ratio of oscillated to unoscillated events (the best signal to noise ratio) when compared to that of Ref. [11]. Moreover the event rate of Ref. [10] above  $\sim 20$  GeV is about 25 % of that of Ref. [11] (see Fig. 5). Therefore the background of  $\pi^0$  due to NC will be reduced by the same amount, looking for  $\tau \rightarrow e\nu\nu$  decay.

In the following, the beam from Ref. [10] and 5 years of data taking are assumed.

## 4 $\tau$ appearance searches

Tau appearance search is performed on the basis of kinematical identification of the  $\tau$  decay. The  $\tau \rightarrow e\nu\nu$  is the channel favourite for this search due to the low background level and the the good electron identification capabilities of the TRD. It is worth noting that in the region of atmospheric anomaly the oscillation probability is  $50 \div 100$  times higher than expected in NOMAD. As a consequence a much lower background rejection power is required.

In order to check the overall  $NOE$  performances, a complete chain of event simulation and analysis have been performed. Event generators including Fermi motion,  $\tau$  polarization and nuclear rescattering inside the nucleus have been used to simulate deep inelastic, quasi elastic and resonance interactions.

Generated events are processed by a GEANT based MonteCarlo in which calorimeter and TRD geometrical set-up are described in detail, down to a scale of a few  $mm$ . Fiber attenuation length, Birks saturation, photoelectron fluctuations and read-out electronics non linearities for both TRD and calorimeter have been taken into account. DST of processed events ( $\tau \rightarrow e\nu\nu$ ,  $\nu_\mu$  NC and  $\nu_e$  CC) have been produced and analysed.

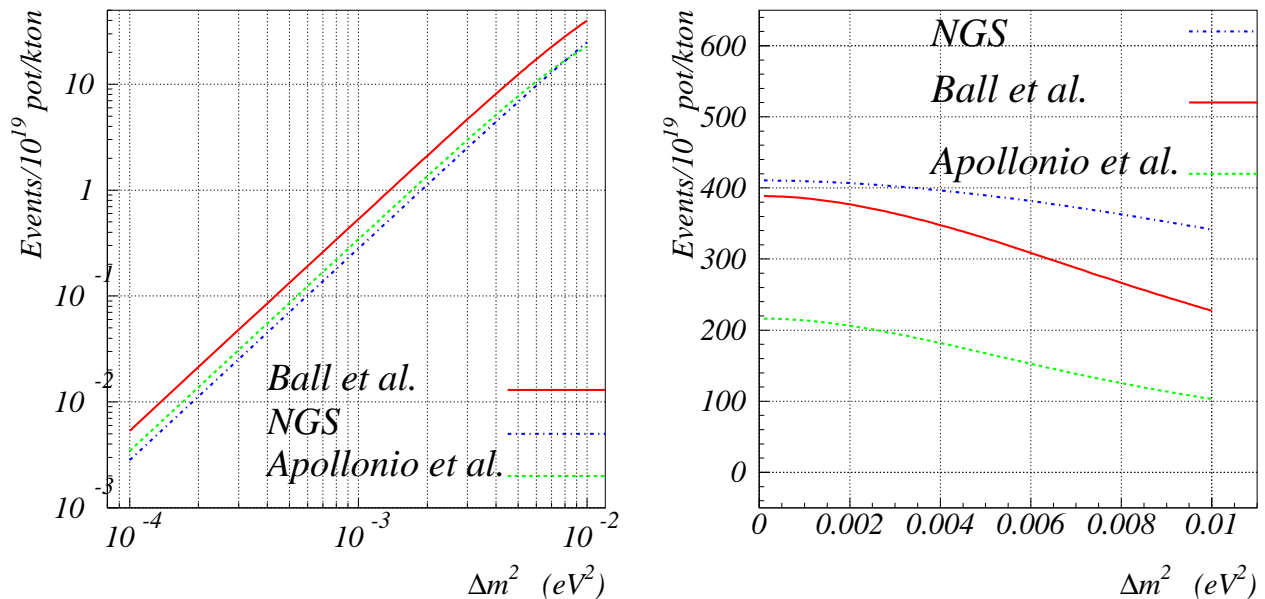


Figure 6: First plot -  $\nu_\tau$  CC interactions for different beams vs  $\Delta m^2$ . Second plot - residual  $\nu_\mu$  CC interactions for different beams vs  $\Delta m^2$ .

Electron identification is performed by looking for high energy releases in the TRD and in the calorimeter elements in fully contained events. The electron candidate is the one that maximizes collected energy in a  $5^\circ$  cone centered at the interaction vertex. Electron direction is reconstructed by weighting hit position with collected energy. With present algorithms an angular resolution of  $0.6^\circ$  and a  $180 \text{ MeV}/c$  resolution on the measurement of transverse momentum are achieved.

The remaining part of the event is used to reconstruct the hadronic component. The obtained resolution on the measurement of transverse momentum is  $420 \text{ MeV}/c$ .

Topological cuts on the electromagnetic shower are applied to reject  $\nu_\mu$  NC events with  $\pi^0$  faking electrons. Work is in progress to improve the reconstruction efficiency and  $\nu_\mu$  NC rejection. Additional cuts are performed to reduce the background:

- the total reconstructed energy  $E_{tot} < 15 \text{ GeV}$ ,
- the electron energy  $E_{e.m.} \geq 1.5 \text{ GeV}$ ,
- the component of electron momentum perpendicular to the hadronic jet direction  $Q_{lep} \geq 0.75 \text{ GeV}/c$ ,
- the transverse mass  $M_T = \sqrt{4p_T^e p_T^m \sin^2(\phi_{e-m}/2)} < 2 \text{ GeV}$ ,
- $\phi_{e-h}$   $\phi_{m-h}$  correlation as shown in Fig. 7.

Analysis cut efficiencies and residual background percentages are reported in Table 1. In Table 2 the expected signal is reported for different values of  $\Delta m^2$ .

## 5 Neural network for the ratio NC/CC

The procedure to perform this measurement is well known [5]. The identification of charged and neutral current events has been improved by means of a neural network.

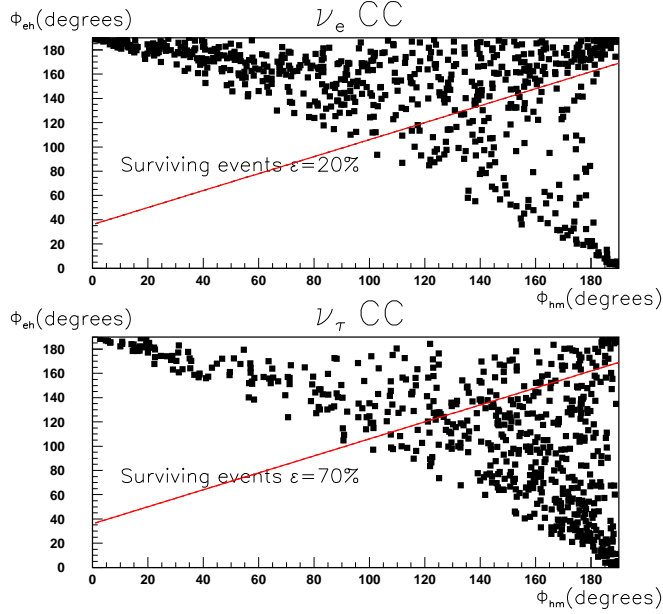


Figure 7: Effects of  $\phi_{e-h}$   $\phi_{m-h}$  cut on background ( $\nu_e$ ) and signal ( $\nu_\tau$ ).

The algorithm uses 24 topological, geometrical and calorimetric event parameters as input. The network has been trained with  $\nu_\mu$  CC and NC MonteCarlo events with a neutrino energy uniformly distributed in the range  $0 \div 50$  GeV. The results of this analysis are shown in Fig. 8.

The  $\mu$  event recognition is mainly dependent on the track length and the NC signal is still affected by a significant CC contamination. We hope to improve the recognition efficiency by tuning the neural network and the input parameters.

## 6 Conclusions

The combined use of two subdetectors (TRD and CAL) allows to search for  $\tau$  appearance signal for events generated in the 2.5 kton TRD target where electron identification, vertex and kinematics reconstruction are performed at best. Nevertheless the whole 8 kton mass can be exploited for disappearance oscillation tests.

Cut	Res. NC	Res. beam $\nu_e$	eff. $\tau \rightarrow e\nu\nu$
Event containment	79 %	67 %	79 %
Track in two views with large released energy	19 %	88 %	91 %
Compact shower starting from the vertex, topology ( $\pi^0$ without initial conversion)	11 %	88 %	89 %
$E_{tot} < 15$ GeV	94 %	45 %	97 %
$E_{e.m.} \geq 1.5$ GeV	55 %	90 %	84 %
$Q_{lep} \geq 0.75$ GeV/c	25 %	75 %	70 %
$M_T < 2$ GeV	57 %	89 %	87 %
$\phi_{e-h}$ $\phi_{m-h}$ correlation	35 %	20 %	70 %

Table 1: Details on analysis cuts, residual background and signal recognition efficiency.



$\Delta m^2$ ( $eV^2$ )	Background events	Signal ( $\tau \rightarrow e\nu\nu$ events)
$5 \times 10^{-3}$	$2.7 \nu_e CC + 1.6 NC = 4.3$	19
$3 \times 10^{-3}$	$2.7 \nu_e CC + 1.9 NC = 4.6$	7
no oscillation	$2.7 \nu_e CC + 2.0 NC = 4.7$	0

Table 2: Estimated background and expected signal in 5 years of data taking ( $1.5 \times 10^{20}$  p.o.t. and 14000  $\nu_\mu$  CC in TRD target).

Such measurements can be carried out at the same time by using an appropriate neutrino beam. The feasibility of both measurements has been demonstrated by means of full analyses. In Fig. 9 the sensitivity of  $NOE$  experiment to  $\nu$  oscillations is shown.

## References

- [1] G. Barbarino *et al.*, INFN/AE-96/11
- [2] G. Barbarino *et al.*, Nucl. Phys. B (Proc. Suppl.) **48** (1996) 204
- [3] G. Osteria *et al.*, Proceedings of the 7th Pisa Meeting on Advanced Detectors, Isola d' Elba, (1997)
- [4] G. Barbarino *et al.*, Proceedings of TAUP97, Gran Sasso Laboratory, (1997) 223
- [5] G. Barbarino *et al.*, INFN/AE-98/09 (also available in <http://www1.na.infn.it/wsubnucl/accel/noe/post/jan98>)
- [6] W.W.M. Allison *et al.* (Soudan 2 Collaboration), Phys. Lett. B **391** (1997) 491
- [7] M. Ambrosio *et al.* (MACRO Collaboration), hep-ex/9807005
- [8] Y. Fukuda *et al.* (SuperKamiokande Collaboration), hep-ex/9807003
- [9] M. Apollonio *et al.* (Chooz Collaboration), Phys. Lett. B **420** (1998) 397
- [10] A.E. Ball, S. Katsanevas and N. Vassilopoulos, Nucl. Instr. Meth. A **383** (1996) 277
- [11] K. Elsener (*ed.*) "The CERN neutrino beam to Gran Sasso", CERN 98/02 and INFN/AE-98/05
- [12] M. Apollonio *et al.*, Addendum to the Expression of Interest to the Gran Sasso Scientific Committee "Studies for a long baseline accelerator and atmospheric neutrino oscillation experiment at Gran Sasso" (1998)

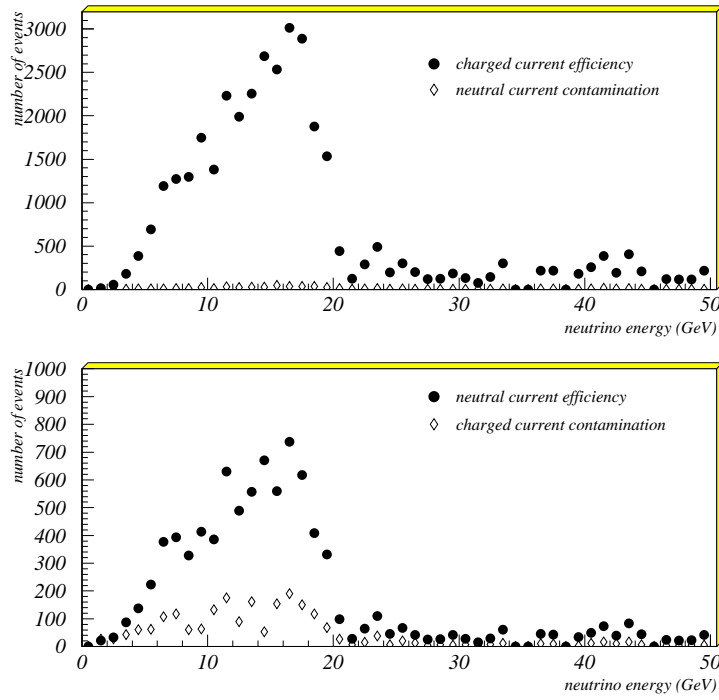


Figure 8: CC and NC signal. The contamination is also shown.

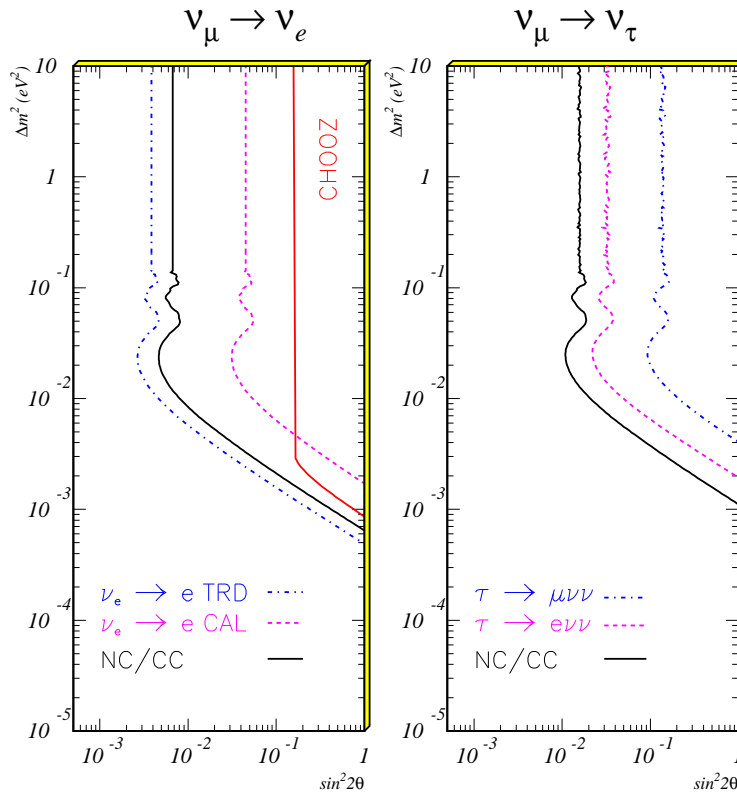


Figure 9:  $NOE$  sensitivity to  $\nu$  oscillations.